Quantum Physics Letters
An International Journal

http://dx.doi.org/10.18576/qpl/090201

Double Spin Asymmetries in Elastic e-d Scattering and Their Sensitivity to the Deuteron's D-Wave Component

H. M. Al-Ghamdi[1], *R. A. Almoerfi*[2], *A. S. Alofi*[2], *and E. M. Darwish*[2,3*]

[1]Physics Department, College of Science, Princess Nourah bint Abdulrahman University, Riyadh 11671, Saudi Arabia
[2]Physics Department, College of Science, Taibah University, Medina 41411, Saudi Arabia
[3]Physics Department, Faculty of Science, Sohag University, Sohag 82524, Egypt

Received: 12 June 2020, Revised: 5 July 2020, Accepted: 15 July 2020
Published online: 1 August 2020

Abstract: We present a calculation for the beam-vector-deuteron double spin asymmetries T_{10}^e and T_{11}^e in elastic electron-deuteron (e-d) scattering as functions of the four-momentum transfer square Q^2 and the electron scattering angle in the laboratory frame θ_e. Our formalism, based on the one-photon-exchange Born approximation, uses the realistic and hight-precision Argonne v18 NN potential for the deuteron wave function and the standard dipole fit for the free nucleon form factors. We also study the sensitivity of our results to the D-wave component of the deuteron wave function. We find large sensitivity of the results for T_{10}^e and T_{11}^e to the D-wave component of the deuteron wave function at $Q^2 > 0.6$ (GeV/c)^2.

Keywords: Elastic electron scattering, Deuteron, Electromagnetic form factors, Nucleon-nucleon interactions, Spin observables

1 Introduction

During the recent years, there is widespread condense that Quantum Chromodynamics (QCD) is the correct theory of strong interactions. On the level of unpolarized differential and total cross sections the theory has been tested with considerable precision by many experiments. However, after about 10 years of intense theoretical and experimental activities in studying the polarized nucleon, the angular momentum composition of the nucleon remains a territory with blank spots. Therefore, high precision data in a large kinematic domain are required to fully explore the spin structure of QCD.

A great potential to achieve an even deeper understanding of the nucleon spin structure may arise from a comprehensive, generalized analysis of many different electromagnetic processes based on realistic approaches. The study of spin-dependent observables has the potential to enhance our understanding of nucleon and nuclear structure. A study of electromagnetic structure of the deuteron, the simplest nucleon system, provides with important information about nucleon-nucleon (NN) interaction. The deuteron has a total spin $S = 1$ and isotopic spin $I = 0$; its electromagnetic structure is, therefore, described by three form factors: the charge monopole $G_C^d(Q^2)$, charge quadrupole $G_Q^d(Q^2)$, and magnetic dipole $G_M^d(Q^2)$ [1,2], where Q^2 is the four-momentum transfer square by electron to the deuteron. Due to smallness of the fine structure constant $\alpha = 1/137$ the form factors are usually extracted from experimentally measurable observables in the framework of Born approximation (one-photon exchange, OPE).

During the last decades, there are many theoretical and experimental studies to investigate the elastic electron-deuteron (e-d) elastic scattering process with polarization effects have been developed [3,4,5,6,7,8,9,10,11,12,13,14,15,16,17]. The deuteron can be used to a good approximation as an effective neutron target (see, for example, Refs. [18,19] and references therein). Elastic e-d scattering process is of fundamental interest with respect to the following important reasons: (i) used to investigate the structure of the two-nucleon system and its electromagnetic properties, (ii) gives valuable information about the properties of the strong interactions in the two-nucleon system, and (iii) provides complementary information on the half-off-shell and full-off-shell behaviors of the NN system.

* Corresponding author e-mail: darwish@science.sohag.edu.eg

Most recently, the influence of the deuteron's D-wave component on (i) vector polarizations of final deuteron P_x and P_z and (ii) tensor-deuteron spin asymmetries T_{20}, T_{21}, and T_{22} in elastic e-d scattering has been investigated in Refs. [16] and [17], respectively. It was found that the results for P_x, P_z, T_{20}, T_{21}, and T_{22} at $Q^2 > 0.5$ (GeV/c)^2 are sensitive to the D-wave component of the deuteron wave functions (DWFs). The sensitivity of $\gamma d \to \pi^0 d$ observables near threshold to the D-wave component of the DWF has also been studied in Refs. [20,21,22], and a significant role of the D-wave component on most of polarization observables was obtained.

In what follows, we calculate the beam-vector-deuteron double spin asymmetries T_{10}^e and T_{11}^e in the elastic e-d scattering process and study their sensitivity to the D-wave component of the DWF. For the NN potential model adapted for the DWF, we consider the realistic and high-precision Argonne $v18$ (AV18) [23] potential. For the free-nucleon electromagnetic form factors, we use the standard dipole fit for the proton and neutron form factors (DFF) from Ref. [5].

In the next section, we will describe the general formalism for the elastic e-d scattering process. The explicit expressions of the beam-vector-deuteron double spin asymmetries T_{10}^e and T_{11}^e are also presented. Section 3 will deal with the main results and discussion. Finally, we conclude our results in Sect. 4.

2 Formalism for Elastic e-d Scattering

In this section, we briefly outline the formalism used in the present work to describe the elastic e-d scattering process. In the mechanism of one-photon-exchange Born approximation (OPEBA), the differential cross section for the elastic scattering of unpolarized electrons of initial (final) energy E (E') from an unpolarized deuteron target with internal structure can be written, neglecting the electron mass, as [24]

$$\frac{d\sigma_0}{d\Omega_e} = \left(\frac{d\sigma}{d\Omega}\right)_{Mott} \frac{E'}{E}\left[A(Q^2) + B(Q^2)\tan^2\frac{\theta_e}{2}\right], \qquad (1)$$

where θ_e is the electron scattering angle in the laboratory frame, $Q^2 = 4EE'\sin^2(\theta_e/2)$, and $(\frac{d\sigma}{d\Omega})_{Mott}$ is the Mott cross-section which is given by

$$\left(\frac{d\sigma}{d\Omega}\right)_{Mott} = \left[\frac{\alpha\cos(\theta_e/2)}{2E\sin^2(\theta_e/2)}\right]^2. \qquad (2)$$

In the case of very low momentum transfer and small scattering angle, the magnetic contribution to the scattering process is suppressed and a precise separation of the form factors using the conventional Rosenbluth method (see Eq. (1)) [25] is not possible. However, their interference provides an easily measurable asymmetry when using a beam of polarized electrons in concert with a polarized deuteron target.

The unpolarized elastic structure functions $A(Q^2)$ and $B(Q^2)$ allow us to create a phenomenological description of the underlying structure of the deuteron. These structure functions can be written in terms of the deuteron elastic form factors as [4]

$$A(Q^2) = [G_C^d(Q^2)]^2 + \frac{8}{9}\tau_d^2[G_Q^d(Q^2)]^2 + \frac{2}{3}\tau_d[G_M^d(Q^2)]^2 \qquad (3)$$

$$B(Q^2) = \frac{4}{3}\tau_d(1+\tau_d)[G_M^d(Q^2)]^2, \qquad (4)$$

where $\tau_d = Q^2/(4M_D^2)$ with M_D is the deuteron mass. In unpolarized elastic e-d scattering experiments, the structure functions $A(Q^2)$ and $B(Q^2)$ can only be measured by determining $B(Q^2)$ directly from the backward scattering cross-section. Equation (4) yields the magnetic form factor $G_M^d(Q^2)$, but the electric monopole $G_C^d(Q^2)$ and the electric quadrupole $G_Q^d(Q^2)$ form factors cannot be separated in Eq. (3). Therefore, one needs an additional third observable to get information on all three deuteron form factors separately. The third observable of choice is the dependence of the scattering on the deuteron polarization.

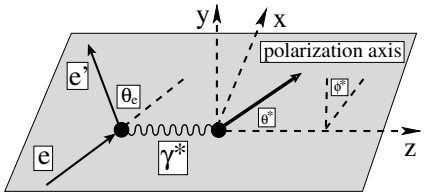

Fig. 1: Conventions of the scattering plane in the elastic e-d scattering process.

Due to its spin 1, the deuteron can be vector and tensor polarized. While in the OPEBA, vector polarization only occurs for polarized electrons [26], tensor polarization exists even if the electron is unpolarized. The differential cross-section for elastic scattering of a longitudinally polarized electron beam from a polarized deuteron target is given in the laboratory frame by [2]

$$\frac{d\sigma}{d\Omega_e}(h, P_z, P_{zz}) = \Sigma(\theta^*, \phi^*) + h\Delta(\theta^*, \phi^*), \qquad (5)$$

where $h = \pm\frac{1}{2}$ is the helicity of the incident electron beam and P_z is the projection of the spin in the direction of the electron three-momentum. P_{zz} are the degree of vector and tensor polarization of the deuteron target. The polarization direction of the deuteron is defined by the polar and azimuthal deuteron spin angles θ^* and ϕ^* in the frame where the z-axis is along the direction of the virtual photon and the y-axis is defined by the vector product of the incoming and the outgoing electron momenta. This is illustrated in Fig. 1.

The first term on the right-hand side in Eq. (5) gives the cross section for an unpolarized electron but a polarized deuteron target and contains the tensor-deuteron asymmetries T_{20}, T_{21}, and T_{22}, which may be written as

$$\Sigma(\theta^*, \phi^*) = \frac{d\sigma_0}{d\Omega_e}\left[1 + \Gamma(\theta^*, \phi^*)\right], \qquad (6)$$

where $\frac{d\sigma_0}{d\Omega_e}$ is the unpolarized differential cross-section given in Eq. (1) and $\Gamma(\theta^*,\phi^*)$ is given by

$$\Gamma(\theta^*,\phi^*) = P_{zz}\Big[\frac{1}{\sqrt{2}}P_2^0(\cos\theta^*)\,T_{20}(Q^2,\theta_e) - \frac{1}{\sqrt{3}}P_2^1(\cos\theta^*)\cos\phi^*\,T_{21}(Q^2,\theta_e) + \frac{1}{2\sqrt{3}}P_2^2(\cos\theta^*)\cos 2\phi^*\,T_{22}(Q^2,\theta_e)\Big]. \quad (7)$$

The second term on the right-hand side in Eq. (5) gives the helicity-dependent differential cross section for a polarized electron beam and a polarized deuteron target. It contains the beam-vector-deuteron double spin asymmetries (T_{10}^e and T_{11}^e) and is given by

$$h\Delta(\theta^*,\phi^*) = \frac{d\sigma_0}{d\Omega}hP_z\Big[\frac{\sqrt{3}}{2}P_1(\cos\theta^*)\,T_{10}^e(Q^2,\theta_e) - \sqrt{3}P_1^1(\cos\theta^*)\cos\phi^*\,T_{11}^e(Q^2,\theta_e)\Big], \quad (8)$$

where the Legendre polynomials $P_\ell(x)$ and the associated Legendre polynomials $P_\ell^m(x)$ are taken according to the Edmonds convention [27].

Following the convention of Ref. [28], the tensor-deuteron (T_{20}, T_{21}, and T_{22}) and the beam-vector-deuteron (T_{10}^e and T_{11}^e) asymmetries can be calculated in terms of the three deuteron electromagnetic form factors $G_C^d(Q^2)$, $G_Q^d(Q^2)$, and $G_M^d(Q^2)$ [4,5,26]. In the present work, we focus on the beam-vector-deuteron double spin asymmetries $T_{10}^e(Q^2,\theta_e)$ and $T_{11}^e(Q^2,\theta_e)$ which are given as follows [29]

$$T_{10}^e(Q^2,\theta_e) = \sqrt{\frac{2}{3}}\frac{\tau_d}{S(Q^2,\theta_e)}\sqrt{(1+\tau_d)\Big[1+\tau_d\sin^2\Big(\frac{\theta_e}{2}\Big)\Big]} \times [G_M^d(Q^2)]^2\tan\Big(\frac{\theta_e}{2}\Big)\sec\Big(\frac{\theta_e}{2}\Big), \quad (9)$$

and

$$T_{11}^e(Q^2,\theta_e) = \frac{2}{\sqrt{3}}\frac{1}{S(Q^2,\theta_e)}\sqrt{\tau_d(1+\tau_d)}\,G_M^d(Q^2) \times\Big[G_C^d(Q^2)+\frac{\tau_d}{3}G_Q^d(Q^2)\Big]\tan\Big(\frac{\theta_e}{2}\Big), \quad (10)$$

where

$$S(Q^2,\theta_e) = A(Q^2)+B(Q^2)\tan^2(\theta_e/2). \quad (11)$$

In the nonrelativistic impulse approximation description of *e-d* scattering, the electron interacts with each nucleon in the deuteron via a virtual photon, and the electromagnetic form factors of the interacting nucleon are taken to be the same as those for a free nucleon. Therefore, the deuteron form factors $G_C^d(Q^2)$, $G_Q^d(Q^2)$, and $G_M^d(Q^2)$ depend only on the radial deuteron wave functions and on the free nucleon form factors. These form factors can be written as [30,31]

$$G_C^d(Q^2) = G_E^S(Q^2)\,C_E^d(Q^2), \quad (12)$$

$$G_Q^d(Q^2) = G_E^S(Q^2)\,C_Q^d(Q^2), \quad (13)$$

$$G_M^d(Q^2) = 2G_M^S(Q^2)\,C_S^d(Q^2)+G_E^S(Q^2)\,C_L^d(Q^2), \quad (14)$$

where $G_E^S(Q^2) = G_E^p(Q^2) + G_E^n(Q^2)$ and $G_M^S(Q^2) = G_M^p(Q^2) + G_M^n(Q^2)$ are the charge and the magnetic isoscalar nucleon form factors, respectively, and $G_{E,M}^{p,n}(Q^2)$ represent the electric and magnetic form factors of the proton and the neutron.

Earlier phenomenological models for the nucleon structure are based on the simple assumption that

$$G_M^p(Q^2) = \mu_p G_E^p(Q^2), \quad (15)$$

$$G_M^n(Q^2) = \mu_n G_E^p(Q^2), \quad (16)$$

where $\mu_p = 2.793$ and $\mu_n = -1.913$ denote the proton and the neutron magnetic moments in nuclear magnetons, respectively, and

$$G_E^n(Q^2) = 0. \quad (17)$$

Only the electric proton form factor was parameterized to describe the experimental data. The most important fit relies on the standard dipole form [30]

$$G_E^p(Q^2) = \Big(1+\frac{Q^2}{\Lambda^2}\Big)^{-2}, \quad (18)$$

where Q^2 is given in (GeV/c)^2 and $\Lambda^2 = 0.71$ (GeV/c)^2. The above-mentioned relations for the proton and the neutron form factors are also used in the present work.

The functions $C_E^d(Q^2)$, $C_Q^d(Q^2)$, $C_S^d(Q^2)$, and $C_L^d(Q^2)$ involve overlaps of the DWFs $u(r)$ and $w(r)$, weighted by spherical Bessel functions. The nonrelativistic formulas for these form factors can be calculated from the deuteron $^3S_1$- and $^3D_1$-state wave functions, $u(r)$ and $w(r)$, respectively, and they are given by [32]

$$C_E^d(Q^2) = \int_0^\infty dr\; j_0\Big(\frac{qr}{2}\Big)\Big[u^2(r)+w^2(r)\Big], \quad (19)$$

$$C_Q^d(Q^2) = \frac{3}{\sqrt{2}\tau_d}\int_0^\infty dr\; j_2\Big(\frac{qr}{2}\Big)\Big[u(r)-\frac{w(r)}{\sqrt{8}}\Big]w(r), \quad (20)$$

$$C_S^d(Q^2) = \int_0^\infty dr\Big\{\Big[u^2(r)-\frac{1}{2}w^2(r)\Big]j_0\Big(\frac{qr}{2}\Big) + \frac{1}{2}\Big[\sqrt{2}u(r)w(r)+w^2(r)\Big]j_2\Big(\frac{qr}{2}\Big)\Big\}, \quad (21)$$

$$C_L^d(Q^2) = \frac{3}{2}\int_0^\infty dr\; w^2(r)\Big[j_0\Big(\frac{qr}{2}\Big)+j_2\Big(\frac{qr}{2}\Big)\Big], \quad (22)$$

where $j_0(x)$ and $j_2(x)$ are the spherical Bessel functions of order zero and two, respectively. The normalization condition is

$$\int_0^\infty dr\,[u^2(r)+w^2(r)] = 1. \quad (23)$$

As in Ref. [20], the integrations over the radial deuteron wave functions $u(r)$ and $w(r)$ are carried out numerically in double precision from $r = r_c$ to $r = R$ using the Simpson's rule with a high degree of accuracy, where r_c is the hard-core radius -if any- and R is larger than the range of the nuclear potential. The contribution to the integrations in the asymptotic region, i.e. from

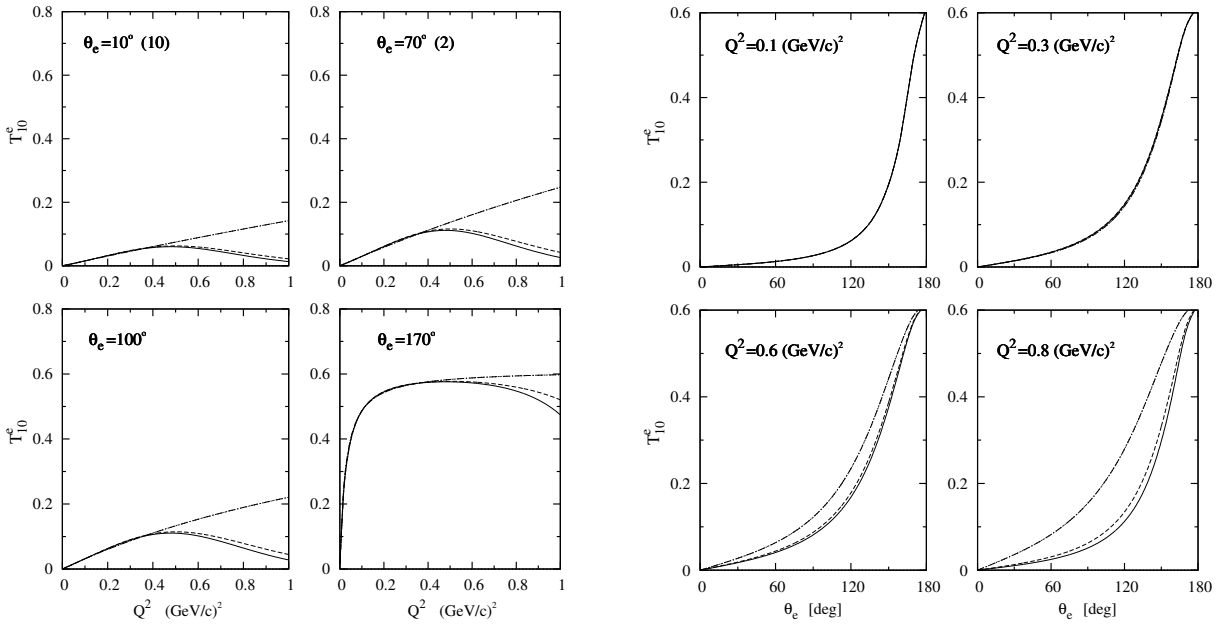

Fig. 2: The beam-vector-deuteron double spin asymmetry T_{10}^e as a function of Q^2 at various fixed values of θ_e (left part) and as a function of θ_e at various fixed values of Q^2 (right part) using the standard dipole fit for nucleon form factors. The solid and dotted curves show the results using the Argonne v18 potential [23] with and without the D-wave component of the DWF, respectively. The dashed and dash-dotted curves represent the results using the Nijmegen-I potential [33] with and without the D-wave component of the DWF, respectively.

$r = R$ to $r = \infty$, is calculated analytically by using the asymptotic forms of the radial DWFs which are given by

$$u(r) \simeq A_S e^{-\gamma r}, \tag{24}$$

$$w(r) \simeq A_D \left(1 + \frac{3}{\gamma r} + \frac{3}{\gamma^2 r^2}\right) e^{-\gamma r}, \tag{25}$$

where A_S and A_D are the asymptotic normalization constants and are called the asymptotic $^3S_1$- and $^3D_1$-state amplitudes of the DWFs, respectively, and γ^2 in fm^{-2} is given by $\gamma^2 = -2mE_b/\hbar^2$ with the reduced n-p mass m and the deuteron binding energy E_b in MeV.

3 Numerical Results and Discussion

Next, we present and discuss the numerical results for the beam-vector-deuteron double spin asymmetries T_{10}^e and T_{11}^e in elastic *e-d* scattering as functions of Q^2 and θ_e. For the DWFs in the initial and final deuteron states, the realistic and high-quality Argonne v18 *NN* potential model [23] is used. For the free proton and neutron electromagnetic form factors, the standard dipole fit from Ref. [5] is used. We also study the sensitivity of the results for the beam-vector-deuteron double spin asymmetries T_{10}^e and T_{11}^e to the deuteron's D-wave component of the DWFs.

The results for the the beam-vector-deuteron double spin asymmetry T_{10}^e are shown in Fig. 2 as a function of

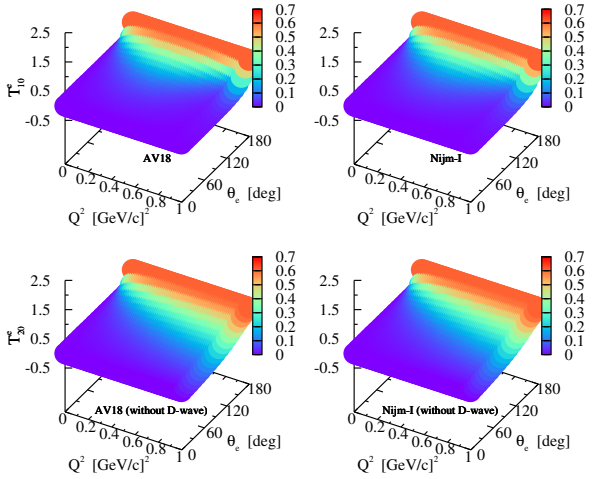

Fig. 3: A three-dimensional plot for the beam-vector-deuteron double spin asymmetry $T_{10}^e(Q^2, \theta_e)$ using the standard dipole fit for nucleon form factors. The upper and lower parts show the results using AV18 (left) and Nijm-I (right) *NN* potentials with and without the D-wave component of the DWF, respectively.

Q^2 at various fixed values of θ_e (left part) and as a function of θ_e at various fixed values of Q^2 (right part) using the standard dipole fit for nucleon form factors from

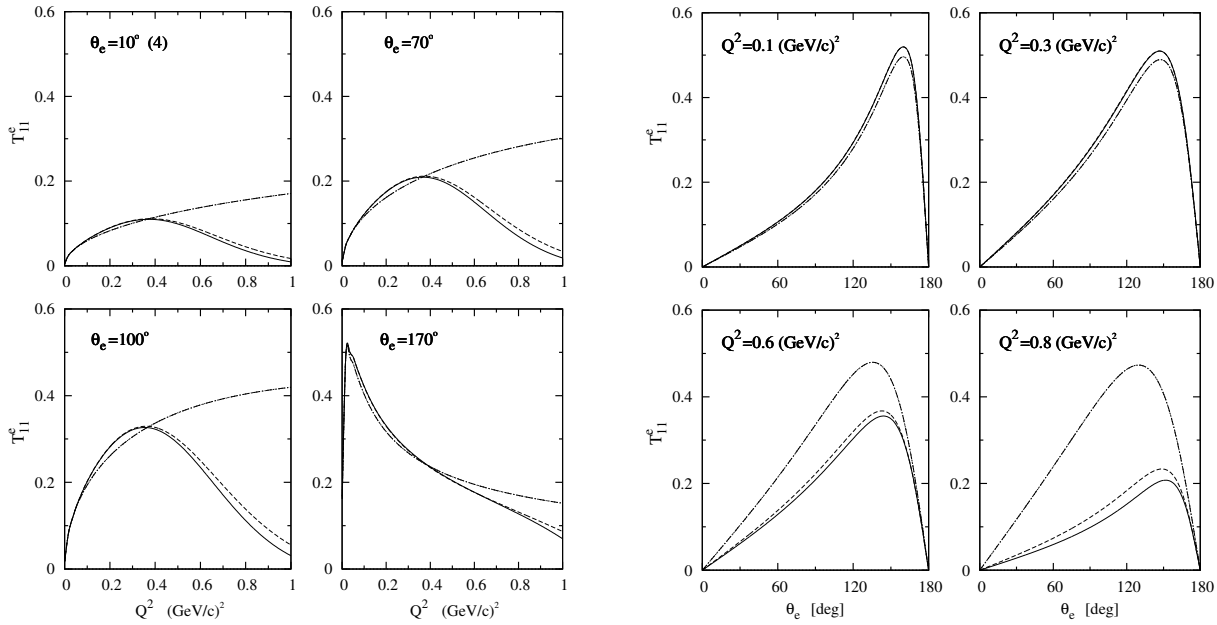

Fig. 4: Same as in Fig. 2 but for the beam-vector-deuteron double spin asymmetry T^e_{11}.

Ref. [5]. The solid and dotted curves in Fig. 2 show the results for T^e_{10} using the realistic Argonne v18 potential [23] with and without the D-wave component of the DWF, respectively. For comparison with the results of other NN potential models, we also present in Fig. 2 the calculations using the DWFs from the realistic Nijmegen-I (Nijm-I) NN potential [33]. These results are displayed in Fig. 2 by the dashed (with D-wave) and dash-dotted (without D-wave) curves.

We see from Fig. 2 that the T^e_{10} asymmetry is positive and vanishes at θ_e=0°. Then, it increases with increasing θ_e until it reaches its maximum at θ_e=180°. We see also that the results for T^e_{10} are slightly dependent on the NN potential models used for the DWFs in particular at $Q^2 < 0.6$ (GeV/c)^2. The results for T^e_{10} using various NN potential models without the D-wave component of the DWF are very close to each others. However, the results for T^e_{10} with both S- and D-wave components of the DWFs are identical for AV19 and Nijm-I NN potentials up to $Q^2 \simeq 0.6$ (GeV/c)^2. At higher values of Q^2, we see small differences between the results for T^e_{10} using AV18 and Nijm-I NN potential models. This means that the results of T^e_{10} are sensitive to only the S-wave component of the DWFs at $Q^2 > 0.6$ (GeV/c)^2.

In Fig. 3 we illustrate three dimensional plots for the beam-vector-deuteron double spin asymmetry T^e_{10} as a function of both Q^2 and θ_e using the standard dipole fit for nucleon form factors from Ref. [5] and the realistic AV18 (left part) and Nijm-I (right part) NN potential models with (upper panels) and without (lower panels) the D-wave component of the DWF. We see that the results for T^e_{10} are slightly dependent on the NN potential model used for the DWF. This dependence increases with increasing both θ_e and Q^2. We found also that the results for T^e_{10} are enhanced by the presence of the D-wave component of the DWF.

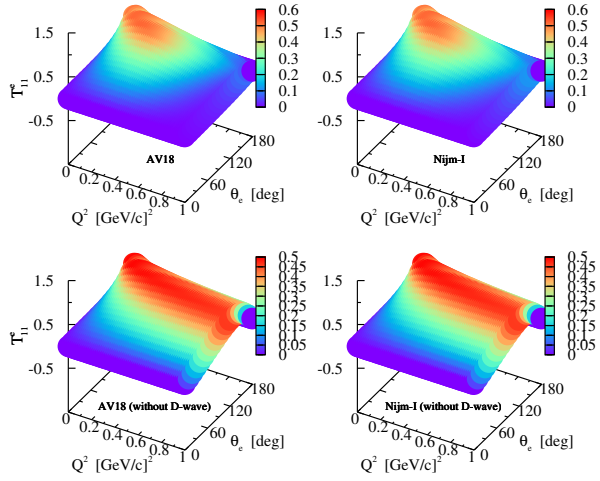

Fig. 5: Same as in Fig. 3 but for the the beam-vector-deuteron double spin asymmetry $T^e_{11}(Q^2, \theta_e)$.

Figure 4 displays the numerical results for the beam-vector-deuteron double spin asymmetry T^e_{11} as a function of Q^2 at various fixed values of θ_e (left part) and as a function of θ_e at various fixed values of Q^2 (right part) using the standard dipole fit for nucleon form factors

from Ref. [5]. The solid and dotted curves in Fig. 4 show the results for T_{11}^e using the realistic Argonne v18 potential [23] with and without the D-wave component of the DWF, respectively. For comparison with the results of other NN potential models, we also present in Fig. 4 the calculations using the DWFs from the realistic Nijmegen-I (Nijm-I) NN potential [33]. These results are displayed by the dashed (with D-wave) and dash-dotted (without D-wave) curves.

We see from Fig. 4 that the results for T_{11}^e are positive and vanish at θ_e=0° and θ_e=π°. We found also that the T_{11}^e asymmetry is slightly dependent on the NN potential models used for the DWFs in particular at $Q^2 < 0.6$ (GeV/c)^2. Indeed, we see that the results for T_{11}^e without the D-wave component of the deuteron wave function are indistinguishable, whereas the results for T_{11}^e with both S- and D-wave components of the DWFs are the same for AV19 and Nijm-I NN potentials up to $Q^2 \simeq 0.6$ (GeV/c)^2. At higher values of Q^2, we see small differences between the results for T_{11}^e using AV18 and Nijm-I NN potential models. This means that the results of T_{11}^e are sensitive to only the S-wave component of the DWFs at $Q^2 > 0.6$ (GeV/c)^2.

Figure 5 shows three dimensional plots for the beam-vector-deuteron double spin asymmetry T_{11}^e as a function of both Q^2 and θ_e using the standard dipole fit for nucleon form factors from Ref. [5] and the realistic AV18 (left part) and Nijm-I (right part) NN potential models with (upper panels) and without (lower panels) the D-wave component of the DWF. We see that the results for T_{11}^e are slightly dependent on the NN potential model used for the DWF. However, the results for T_{11}^e are influenced by the D-wave component of the DWF.

4 Conclusion

In this paper, we have presented a calculation for the beam-vector-deuteron double spin asymmetries T_{10}^e and T_{11}^e in the elastic e-d scattering process as functions of Q^2 and θ_e using an approach which is based on the one-photon-exchange Born approximation. The deuteron wave function used in our computation is obtained from the realistic and hight-precision Argonne v18 NN potential [23]. For the free nucleon form factors, we have taken the standard dipole fit for the proton and neutron form factors [5]. We have also studied the sensitivity of our results for T_{10}^e and T_{11}^e to the D-wave component of the deuteron wave function.

We have obtained positive values for the T_{10}^e and T_{11}^e asymmetries. The former is vanished at θ_e=0° and reached its maximum at θ_e=180°, whereas the latter is vanished at θ_e=0° and θ_e=π°. We find large sensitivity of the results for T_{10}^e and T_{11}^e to the D-wave component of the DWF at $Q^2 > 0.6$ (GeV/c)^2. The results for T_{10}^e and T_{11}^e are found to be enhanced by the presence of the D-wave component of the DWF, because the results with both the S- and the D-wave components are found to be indistinguishable.

Summarizing, we can conclude that the T_{11}^e asymmetry can be used with the unpolarized structure functions $A(Q^2)$ and $B(Q^2)$ to separate the three deuteron electromagnetic form factors $G_C^d(Q^2)$, $G_Q^d(Q^2)$, and $G_M^d(Q^2)$. Therefore, future experimental measurements for the spin asymmetry T_{11}^e are needed for this purpose.

Conflict of Interest

The authors declare that there is no conflict of interest regarding the publication of this article.

References

[1] F. Gross, Phys. Rev. **136**, B140 (1965); R. G. Arnold, C. E. Carlson, and F. Gross, Phys. Rev. C **21**, 1426 (1980).
[2] T. W. Donnelly and A. S. Raskin, Ann. Phys. (N. Y.) **169**, 247 (1986).
[3] J. Carlson and R. Schiavilla, Rev. Mod. Phys. **70**, 743 (1998).
[4] M. Garcon and J. W. Van Orden, Adv. Nucl. Phys. **26**, 293 (2001).
[5] R. Gilman and F. Gross, J. Phys. G **28**, R37 (2002).
[6] E. M. Darwish and M. Y. Hussein, J. Kor. Phys. Soc. **52**, 226 (2008).
[7] E. M. Darwish, M. Y. Hussein and B. Abu Sal, Appl. Math. & Inform. Sci. **3**, 309 (2009).
[8] D. K. Hasell *et al.*, Ann. Rev. Nucl. Part. Sci. **61**, 409 (2011).
[9] L. E. Marcucci *et al.*, J. Phys. G **43**, 023002 (2016).
[10] E. M. Darwish, A. Abd El-Daiem and M. M. Abd El-Wahab, Phys. Part. Nucl. Lett. **14**, 822 (2017); E. M. Darwish, E. M. Mahrous, and F. A. Alhazmi, AIP Conf. Proc. **1976**, 020008 (2018).
[11] V. I. Zhaba, J. Phys. Stud. **21**, 4101 (2017).
[12] E. M. Mahrous, Int. J. New Horz. Phys. **6** (1), 15 (2019).
[13] E. M. Mahrous, E. M. Darwish, H. M. Abou-Elsebaa, and A. Hemmdan, Moscow Uni. Phys. Bull. **74**, 341 (2019); E. M. Mahrous, E. M. Darwish, H. M. Abou-Elsebaa, and A. Hemmdan, Bulg. J. Phys. **46**, 134 (2019).
[14] E. M. Darwish, A. Hemmdan, K. O. Behairy, E. M. Mahrous, Kh. S. Alsadi, and M. A. Hassanain, Moscow Uni. Phys. Bull. **74**, 353 (2019).
[15] E. M. Darwish, H. M. Abou-Elsebaa, E. M. Mahrous, and S. S. Al-Thoyaib, Ind. J. Phys. **94**, 1025 (2020).
[16] H. M. Al-Ghamdi, E. S. Almogait, M. J. Al-Salah, and E. M. Darwish, Int. J. New Horz. Phys. **7**, 47 (2020).
[17] E. M. Darwish, R. A. Almoerfi, and A. E. Elmeshneb, Int. J. New Horz. Phys. **7**, 55 (2020).
[18] E. M. Darwish, *Incoherent Pion Photoproduction on the Deuteron: A Review* (LAMBERT Academic Publishing, 2015).
[19] E. M. Darwish and H. Mansour, *π-Production off Deuteron Near η-Threshold: A Theoretical Overview* (LAMBERT Academic Publishing, 2015).
[20] E.M. Darwish and M. Saleh Yousef, Moscow Univ. Phys. Bull. **74**, 595 (2019).

[21] H. M. Al-Ghamdi, E. S. Almogait, E. M. Darwish, and S. Abdel-Khalek, Braz. J. Phys. **50**, 615 (2020).
[22] E.M. Darwish, H. M. Abou-Elsebaa, Kh. S. Alsadi, and M. Saleh Yousef, Moscow Univ. Phys. Bull. **75**, 198 (2020).
[23] R. B. Wiringa, V. G. J. Stoks and R. Schiavilla, Phys. Rev. C **51**, 38 (1995).
[24] F. Gross, Phys. Rev. **142**, 1025 (1966); F. Gross, Phys. Rev. **152** (E), 1517 (1966).
[25] M. N. Rosenbluth, Phys. Rev. **79**, 615 (1950).
[26] R. G. Arnold, C. E. Carlson, and F. Gross, Phys. Rev. C **23**, 363 (1981).
[27] A. R. Edmonds, *Angular Momentum in Quantum Mechanics* (Princeton University Press, 1968).
[28] S. E. Darden, in *Polarization Phenomena in Nuclear Physics*, edited by H. H. Barschall and W. Haeberli (The University of Wisconsin Press, Madison, Wisconsin, 1971).
[29] P. J. Karpius, PhD dissertation, University of New Hampshire, (2005).
[30] M. I. Haftel, L. Mathelitsch and H. F. K. Zingl, Phys. Rev. C **22**, 1285 (1980).
[31] J. Arrington, C. D. Roberts, and J. M. Zanotti, J. Phys. G **34**, S23 (2007).
[32] V. Jankus, Phys. Rev. **102**, 1586 (1956).
[33] V. G. J. Stoks *et al.*, Phys. Rev. C **49**, 2950 (1994).